Journal of Computational Physics **183,** 652–675 (2002)
doi:10.1006/jcph.2002.7210

Simplified P_N Approximations to the Equations of Radiative Heat Transfer and Applications[1]

Edward W. Larsen,* Guido Thömmes,† Axel Klar,†
Mohammed Seaïd,† and Thomas Götz‡

*Department of Nuclear Engeneering and Radiological Sciences, University of Michigan, Ann Arbor, Michigan 48109-2104; †Department of Mathematics, Technical University of Darmstadt, 64289 Darmstadt, Germany; and ‡Department of Mathematics, University of Kaiserslautern, 63000 Kaiserslautern
E-mail: edlarsen@engin.umich.edu, thoemmes@mathematik.tu-darmstadt.de, klar@mathematik.tu-darmstadt.de, seaid@mathematik.tu-darmstadt.de, goetz@mathematik.uni-kl.de

Received February 2, 2002; revised September 13, 2002

Simplified P_N (SP_N) approximations to the equations of radiative heat transfer are derived for optically thick, diffusive systems, and appropriate boundary conditions are formulated. The SP_N equations are derived by an asymptotic analysis, while the boundary conditions are obtained from a variational analysis. Numerical comparisons of the SP_N, equilibrium diffusion, and full transport equations are presented to demonstrate the accuracy and efficiency of the SP_N approximations.

1. INTRODUCTION

Radiative transfer equations are used in many applications, for example, to describe cooling down of molten glass or heat transfer in gas turbines. In glass manufacturing, a hot melt of glass is cooled down to room temperature. This annealing must be monitored carefully to avoid excessive temperature differences, which may affect the quality of the product or even lead to cracking. To control the annealing process, the radiative transfer equations may be used to predict accurately the temperature evolution in the glass. These equations involve the direction-dependent thermal radiation field, because a significant part of the energy is transported by photons. Unfortunately, this makes the numerical solution of the radiative transfer equations complicated and expensive, particularly in higher spatial dimensions. (Besides the spatial, time, and frequency variables, the directional variables also must be included, giving a 7-dimensional phase space.) Thus, approximations of the

[1] This work was supported by DFG, Grant KL 1105/7 and DFG, SFB 568.

0021-9991/02 $35.00

full radiation transport model that are computationally less time consuming, yet sufficiently accurate, are of great practical interest.

A widely used approximation to radiative transfer is the spherical harmonic, or P_N approximation. A major drawback of this approximation for complicated problems in higher spatial dimensions is the large number and complexity of equations that must be solved. In this paper, we propose the simpler SP_N approximations as alternatives to the P_N equations. The SP_N approximation is based on coupled systems of diffusion (elliptic) equations that depend on space, time, and frequency (not direction). The number and complexity of the SP_N equations are considerably reduced compared to the P_N equations. See [16] for the P_N equations in the considered context.

The SP_N method was introduced in 1961 by Gelbard in the field of nuclear reactor theory [4]. For many years, this method suffered from a lack of theoretical foundation, with the result that it was not completely accepted in the technical community. However, this has been remedied during the last decade by the work of one of the authors of this paper, amongst others, such that the method has now been substantiated [1, 8].

To model glass cooling, we consider the following radiative transfer problem. For a point x in the domain $V \subset \mathbb{R}^3$, we have the *energy balance equation*

$$c_m \rho_m \frac{\partial T}{\partial t} = \nabla \cdot k \nabla T - \int_{\nu_1}^{\infty} \int_{S^2} \kappa (B - I)\, d\Omega\, d\nu, \tag{1.1a}$$

and the *equation of transfer*

$$\forall \nu > \nu_1, \Omega \in S^2 : \quad \frac{1}{c} \frac{\partial I}{\partial t} + \Omega \cdot \nabla I = \kappa (B - I). \tag{1.1b}$$

On the boundary, $x \in \partial V$, the incident radiation is prescribed by the *semi-transparent* boundary condition

$$I(\Omega, \nu) = \rho (n \cdot \Omega) I(\Omega', \nu) + [1 - \rho (n \cdot \Omega)] B(\nu, T_b), \quad \forall n \cdot \Omega < 0, \tag{1.1c}$$

where

$$\Omega' = \Omega - 2(n \cdot \Omega) n$$

is the specular reflection of Ω off the surface ∂V, and the temperature satisfies

$$k n \cdot \nabla T = h(T_b - T) + \alpha \pi \left(\frac{n_2}{n_1} \right)^2 \int_0^{\nu_1} [B(\nu, T_b) - B(\nu, T)]\, d\nu. \tag{1.1d}$$

At initial time $t = 0$, the temperature is prescribed by

$$T(x, 0) = T_0(x), \quad x \in V. \tag{1.1e}$$

In the above equations, $I(x, t, \Omega, \nu)$ denotes the specific intensity of radiation at point $x \in V$, traveling in direction $\Omega \in S^2$, with frequency $\nu > \nu_1$, at time $t \geq 0$; and $T(x, t)$ denotes the material temperature, for $x \in V$ and $t \geq 0$. At the exterior boundary ∂V between the glass and surrounding air, with refractive indices $n_1 > n_2$, respectively, light rays are

reflected and refracted. This is modeled by the semi-transparent boundary condition (1.1c), the physics of which is described next.

At points x exterior to V and for directions Ω pointing toward V, photon radiation exists in a Planckian distribution $B(\nu, T_b)$ at specified temperature T_b. Thus, a point x just outside of V observes this Planckian radiation, for all *incident* directions (all directions Ω satisfying $\Omega \cdot n < 0$, where n is the unit outer normal).

On ∂V, a specified fraction [the *reflectivity* $\rho(n \cdot \Omega)$, defined below] of the above incident radiation is specularly reflected back into the exterior of V, while the remaining fraction, $1 - \rho(n \cdot \Omega)$, penetrates through ∂V into V. The same physics applies to photons inside V that attempt to leak out through ∂V.

Thus, a point x just inside of ∂V sees, for incident directions Ω, the *penetrating* radiation described above,

$$I_p(\Omega, \nu) \equiv [1 - \rho(n \cdot \Omega)]B(\nu, T_b) \tag{1.2a}$$

plus the *reflected* radiation, which in the process of attempting to leak out through ∂V is specularly reflected back into V:

$$I_r(\Omega, \nu) \equiv \rho(n \cdot \Omega)I(\Omega', \nu). \tag{1.2b}$$

The sum $I_r + I_p$ constitutes the right side of Eq. (1.1c). This boundary condition holds for points x just *inside* of ∂V.

The initial temperature is prescribed by Eq. (1.1e), and the boundary condition for the T is given by Eq. (1.1d). The integration in the second term of this equation is performed on the *opaque* interval of the spectrum $[0, \nu_1]$, where radiation is completely absorbed.

Equations (1.1) also contain the speed of light c, the *opacity* $\kappa(\nu)$, the heat conductivity k, the convective heat transfer coefficient h, the specific heat c_m, the density ρ_m, and the Planck function

$$B(\nu, T) = n_1^2 \frac{2h_P\nu^3}{c^2}\left(e^{\frac{h_P\nu}{k_BT}} - 1\right)^{-1}$$

for black body radiation in glass. The Planck function involves Planck's constant h_P, Boltzmann's constant k_B, and the speed of light in vacuum c. For industrial glass-cooling problems, the $1/c$ term in Eq. (1.1b) is negligible and is not included in the remainder of paper. (Effectively, the speed of photons is approximated as ∞.)

The *reflectivity* $\rho \in [0, 1]$ is the proportion of radiation that is reflected. It is equal to 1 if total reflection occurs, i.e., if $\theta_1 > \theta_c$, where θ_c is the *critical angle* given by $\sin\theta_c = n_2/n_1$. Otherwise, ρ is calculated according to Fresnel's equation

$$\rho(\mu) = \frac{1}{2}\left[\frac{\tan^2(\theta_1 - \theta_2)}{\tan^2(\theta_1 + \theta_2)} + \frac{\sin^2(\theta_1 - \theta_2)}{\sin^2(\theta_1 + \theta_2)}\right],$$

where the *refraction angles* θ_1 and θ_2 are given by $\cos\theta_1 = |n \cdot \Omega| = \mu$ and Snell's law of refraction

$$n_1 \sin\theta_1 = n_2 \sin\theta_2.$$

Finally, the *hemispheric emissivity* α of the boundary surface in (1.1d) is related to the reflectivity ρ by

$$\alpha = 2n_1 \int_0^1 [1 - \rho(\mu)]\, d\mu.$$

If $T_b =$ constant, then a steady-state *equilibrium* solution of the above problem is $T(x, t) = T_b$ and $I(x, t, \Omega, \nu) = B(\nu, T_b)$. This solution is the $t \to \infty$ limit of a problem in which the initial temperature $T_0(x)$ inside the glass differs from T_b.

For more detailed discussions of these equations and applications in glass manufacturing problems, we refer the reader to [6, 7, 9, 16] and monographs [5, 12].

In this paper we study *optically thick* problems, in which the opacity κ is large and the radiation propagates mainly in a diffusion-like manner. To introduce the proper scalings, we rewrite the above equations in dimensionless form, introducing reference values that correspond to typical values of the physical quantities. We impose the relations

$$t_{ref} = c_m \rho_m \kappa_{ref} x_{ref}^2 \frac{T_{ref}}{I_{ref}} \quad \text{and} \quad k_{ref} = \frac{I_{ref}}{\kappa_{ref} T_{ref}}$$

on these reference values and define the dimensionless parameter

$$\varepsilon = \frac{1}{\kappa_{ref} x_{ref}}, \tag{1.3}$$

which satisfies $0 < \varepsilon \ll 1$ in the optically thick, diffusive regime. The rescaled equations read (without marking the scaled quantities)

$$\varepsilon^2 \frac{\partial T}{\partial t} = \varepsilon^2 \nabla \cdot k \nabla T - \int_{\nu_1}^{\infty} \int_{S^2} \kappa (B - I)\, d\Omega\, d\nu, \tag{1.4a}$$

$$\forall \nu > \nu_1, \Omega \in S^2: \quad \varepsilon \Omega \cdot \nabla I = \kappa (B - I). \tag{1.4b}$$

The boundary condition for the temperature becomes

$$\varepsilon k\, n \cdot \nabla T = h(T_b - T) + \alpha \pi \left(\frac{n_2}{n_1} \right)^2 \int_0^{\nu_1} [B(\nu, T_b) - B(\nu, T)]\, d\nu. \tag{1.4c}$$

The initial condition for the temperature [Eq. (1.1e)] and the boundary condition on the incident intensity [Eq. (1.1c)] are unaffected by this conversion to dimensionless variables.

It is well known that an *outer* asymptotic expansion of Eqs. (1.4a) and (1.4b) leads to the *equilibrium diffusion* or *Rosseland* approximation

$$\frac{\partial T}{\partial t} = \nabla \cdot (k + k_r(T)) \nabla T, \quad \text{with } k_r(T) = \frac{4\pi}{3} \int_{\nu_1}^{\infty} \frac{1}{\kappa} \frac{\partial B}{\partial T}\, d\nu,$$

which is expected to be valid in the interior of V; see e.g. [9, 13, 14]. Unfortunately, this relatively simple diffusion approximation does not describe boundary layers—the regions in which the temperature gradients (and the mechanical stresses in the glass) are greatest. Thus, the question arises whether more sophisticated "diffusion" approximations can model the boundary layers at the outer boundary and internal interfaces of the system. In the realm

of neutron transport, such higher-order asymptotic corrections to diffusion theory exist and are reasonably well understood; they are the *Simplified* P_N (SP_N) theories mentioned above [1, 4, 8, 15]. Although these theories are diffusive in nature, they describe boundary layers and can be remarkably more accurate than the standard diffusion approximation for neutrons. In this paper, we adopt some of the SP_N concepts from neutronics to the problem of photon transport and annealing in glass.

For other approximate theories for the above radiative transfer equations, and applications, see for example [3, 11].

The remainder of this paper is organized as follows. In Section 2, the *outer* asymptotic expansion to Eqs. (1.4a) and (1.4b) is performed. The resulting approximations consist of replacing Eq. (1.4b) by one or more SP_N equations, in which the angular variable Ω is eliminated (but the frequency variable ν is not eliminated). These frequency-dependent diffusion equations are coupled to each other and to the frequency-independent heat transfer equation (1.4a). In Section 3, boundary conditions for the SP_N equations are formulated from a variational analysis. (The SP_N equations themselves can be derived variationally, as well as asymptotically, but this process is very laborious [1, 14, 15].) Sections 4 and 5 contain 1-D and multi-D numerical simulations, which demonstrate the accuracy and efficiency of the SP_N apaproximations. We conclude this paper with a discussion in Section 6.

2. ASYMPTOTIC DERIVATION OF THE SP_N EQUATIONS

To solve Eq. (1.4b) in domain V, we write this equation as

$$\left(1 + \frac{\varepsilon}{\kappa}\Omega \cdot \nabla\right) I(x, t, \Omega, \nu) = B(\nu, T)$$

and apply Neumann's series to formally obtain

$$\begin{aligned} I &= \left(1 + \frac{\varepsilon}{\kappa}\Omega \cdot \nabla\right)^{-1} B \\ &\cong \left[1 - \frac{\varepsilon}{\kappa}\Omega \cdot \nabla + \frac{\varepsilon^2}{\kappa^2}(\Omega \cdot \nabla)^2 - \frac{\varepsilon^3}{\kappa^3}(\Omega \cdot \nabla)^3 + \frac{\varepsilon^4}{\kappa^4}(\Omega \cdot \nabla)^4 \cdots\right] B. \end{aligned} \tag{2.1}$$

Integrating with respect to Ω and using

$$\int_{S^2} (\Omega \cdot \nabla)^n \, d\Omega = [1 + (-1)^n] \, \frac{2\pi}{n+1} \nabla^n,$$

where $\nabla^2 = \nabla \cdot \nabla = \Delta$ is the spatial Laplacian, we obtain

$$\varphi = \int_{S^2} I \, d\Omega = 4\pi \left[1 + \frac{\varepsilon^2}{3\kappa^2}\nabla^2 + \frac{\varepsilon^4}{5\kappa^4}\nabla^4 + \frac{\varepsilon^6}{7\kappa^6}\nabla^6 \cdots\right] B + \mathcal{O}(\varepsilon^8).$$

Hence,

$$4\pi B = \left[1 + \frac{\varepsilon^2}{3\kappa^2}\nabla^2 + \frac{\varepsilon^4}{5\kappa^4}\nabla^4 + \frac{\varepsilon^6}{7\kappa^6}\nabla^6\right]^{-1}\varphi + \mathcal{O}(\varepsilon^8)$$
$$= \left\{1 - \left[\frac{\varepsilon^2}{3\kappa^2}\nabla^2 + \frac{\varepsilon^4}{5\kappa^4}\nabla^4 + \frac{\varepsilon^6}{7\kappa^6}\nabla^6\right] + \left[\frac{\varepsilon^2}{3\kappa^2}\nabla^2 + \frac{\varepsilon^4}{5\kappa^4}\nabla^4 + \frac{\varepsilon^6}{7\kappa^6}\nabla^6\right]^2 - \left[\frac{\varepsilon^2}{3\kappa^2}\nabla^2 + \frac{\varepsilon^4}{5\kappa^4}\nabla^4 + \frac{\varepsilon^6}{7\kappa^6}\nabla^6\right]^3 \cdots\right\}\varphi + \mathcal{O}(\varepsilon^8),$$

This directly yields the formal asymptotic equation for φ:

$$\forall \nu > \nu_1: \quad 4\pi B = \left[1 - \frac{\varepsilon^2}{3\kappa^2}\nabla^2 - \frac{4\varepsilon^4}{45\kappa^4}\nabla^4 - \frac{44\varepsilon^6}{945\kappa^6}\nabla^6\right]\varphi + \mathcal{O}(\varepsilon^8). \tag{2.2}$$

Taking terms of $\mathcal{O}(\varepsilon^4)$, $\mathcal{O}(\varepsilon^6)$ or $\mathcal{O}(\varepsilon^8)$ into account and proceeding as shown below, we obtain the SP_1, SP_2, and SP_3 approximations, respectively. These approximations are all independent of Ω and contain frequency ν and time t as parameters.

2.1. SP_1 and Rosseland (Diffusion) Approximations

From Eq. (2.2), we obtain

$$4\pi B = \varphi - \frac{\varepsilon^2}{3\kappa^2}\nabla^2\varphi + \mathcal{O}(\varepsilon^4)$$

which, up to $\mathcal{O}(\varepsilon^4)$, may be written as

$$\forall \nu > \nu_1: \quad -\varepsilon^2\nabla \cdot \frac{1}{3\kappa}\nabla\varphi + \kappa\varphi = \kappa(4\pi B). \tag{2.3a}$$

In this equation, ν is simply a parameter. Also, in the derivation of Eq. (2.2), κ is independent of space, but we have written Eq. (2.3a) as though κ were space-dependent. [A more careful calculation shows that for heterogeneous media (space-dependent κ), Eq. (2.3a) remains asymptotically correct.]

In practice, Eqs. (2.3a) are solved independently for each frequency or frequency group and are subsequently coupled via Eq. (1.4a). By (2.3a),

$$\int_{\nu_1}^{\infty}\int_{S^2} \kappa(B - I)\, d\Omega\, d\nu = \int_{\nu_1}^{\infty} \kappa(4\pi B - \varphi)\, d\nu$$
$$= -\varepsilon^2 \int_{\nu_1}^{\infty} \nabla \cdot \frac{1}{3\kappa}\nabla\varphi\, d\nu + \mathcal{O}(\varepsilon^4).$$

Thus, the energy balance equation (1.4a) becomes, up to $\mathcal{O}(\varepsilon^2)$,

$$\frac{\partial T}{\partial t} = \nabla \cdot k\nabla T + \int_{\nu_1}^{\infty} \nabla \cdot \frac{1}{3\kappa}\nabla\varphi\, d\nu. \tag{2.3b}$$

Equations (2.3a) and (2.3b) are the SP_1 approximation to Eqs. (1.4a) and (1.4b). Initial and boundary conditions for these equations are discussed below in Section 3.

Since (2.3b) has $\mathcal{O}(\varepsilon^2)$ error, the overall SP_1 error is $\mathcal{O}(\varepsilon^2)$. Using $\varphi = 4\pi B + \mathcal{O}(\varepsilon^2)$ [which follows from Eq. (2.3a)] in (2.3b), one obtains up to $\mathcal{O}(\varepsilon^2)$ the simpler equation

$$\begin{aligned}\frac{\partial T}{\partial t} &= \nabla \cdot k \nabla T + \int_{\nu_1}^{\infty} \nabla \cdot \frac{1}{3\kappa} \nabla (4\pi B)\, d\nu \\ &= \nabla \cdot k \nabla T + \nabla \cdot \left(\frac{4\pi}{3} \int_{\nu_1}^{\infty} \frac{1}{\kappa} \frac{\partial B}{\partial T}\, d\nu \right) \nabla T \end{aligned} \tag{2.4}$$

for $T(x, t)$ alone, in which the direction *and* frequency variables have been eliminated. Equation (2.4) is the conventional *equilibrium diffusion* or *Rosseland approximation* to Eqs. (1.4a) and (1.4b).

Equations (2.3) are more complicated and costly to solve than Eq. (2.4) because they contain the frequency variable ν. However, they permit a boundary layer behaviour near the boundary ∂V that is not present in Eq. (2.4). Thus, although Eqs. (2.3) and (2.4) are formally asymptotically equivalent—both having $\mathcal{O}(\varepsilon^2)$ errors—the more complicated SP_1 equations (2.3) contain more transport physics and, in practice, produce more accurate results.

2.2. SP_2 Approximation

From Eq. (2.2), we get for $\varepsilon \ll 1$

$$4\pi B = \varphi - \frac{\varepsilon^2}{3\kappa^2} \nabla^2 \varphi - \frac{4\varepsilon^2}{15\kappa^2} \nabla^2 \left(\frac{\varepsilon^2}{3\kappa^2} \nabla^2 \varphi \right) + \mathcal{O}(\varepsilon^6).$$

This implies

$$\frac{\varepsilon^2}{3\kappa^2} \nabla^2 \varphi = \varphi - 4\pi B + \mathcal{O}(\varepsilon^4).$$

Hence, with $\mathcal{O}(\varepsilon^6)$ error, the expansion above gives

$$4\pi B = \varphi - \frac{\varepsilon^2}{3\kappa^2} \nabla^2 \varphi - \frac{4\varepsilon^2}{15\kappa^2} \nabla^2 [\varphi - 4\pi B] = \varphi - \frac{\varepsilon^2}{3\kappa^2} \nabla^2 \left[\varphi + \frac{4}{5} (\varphi - 4\pi B) \right],$$

or equivalently,

$$-\varepsilon^2 \nabla \cdot \frac{1}{3\kappa} \nabla \left[\varphi + \frac{4}{5} (\varphi - 4\pi B) \right] + \kappa \varphi = \kappa (4\pi B). \tag{2.5}$$

This yields

$$\int_{\nu_1}^{\infty} \int_{S^2} \kappa (B - I)\, d\Omega\, d\nu = -\varepsilon^2 \int_{\nu_1}^{\infty} \nabla \cdot \frac{1}{3\kappa} \nabla \left[\varphi + \frac{4}{5} (\varphi - 4\pi B) \right] d\nu + \mathcal{O}(\varepsilon^4). \tag{2.6}$$

Thus, the energy balance equation (1.4a) becomes, up to $\mathcal{O}(\varepsilon^4)$,

$$\frac{\partial T}{\partial t} = \nabla \cdot k \nabla T + \int_{\nu_1}^{\infty} \nabla \cdot \frac{1}{3\kappa} \nabla \left[\varphi + \frac{4}{5} (\varphi - 4\pi B) \right] d\nu. \tag{2.7}$$

Now, if we define

$$\xi = \varphi + \frac{4}{5}(\varphi - 4\pi B), \tag{2.8}$$

then Eqs. (2.5) and (2.7) become the SP_2 equations:

$$\frac{\partial T}{\partial t} = \nabla \cdot k\nabla T + \int_{\nu_1}^{\infty} \nabla \cdot \frac{1}{3\kappa}\nabla\xi \, d\nu, \tag{2.9a}$$

$$-\varepsilon^2 \nabla \cdot \frac{3}{5\kappa}\nabla\xi + \kappa\xi = \kappa(4\pi B). \tag{2.9b}$$

(Boundary conditions for Eqs. (2.9) are described later in Section 3.) After solving Eqs. (2.9) for ξ and T, ϕ can be found from Eq. (2.8):

$$\varphi = \frac{5}{9}\xi + \frac{4}{9}(4\pi B).$$

The SP_2 equations (2.9) and the SP_1 equations (2.3) are remarkably similar. This is because the SP_1 equations contain some, but not all, of the $\mathcal{O}(\varepsilon^4)$ correction terms. In the realm of neutron transport, the SP_2 approximation has not found favour because, in the presence of material inhomogenities in κ, it yields discontinuous solutions, which are physically unrealistic. However, it is obvious that Eqs. (2.9) cannot produce a discontinuous solution.

Finally, we emphasize that Eqs. (2.9) are an $\mathcal{O}(\varepsilon^4)$ approximation to Eqs. (1.4) if (i) κ is independent of space, or (ii) the entire problem has a planar-geometry space-dependence (including κ). In general multidimensional geometries with space-dependent κ, Eqs. (2.9) are *not* an $\mathcal{O}(\varepsilon^4)$ approximation to Eqs. (1.4) because other $\mathcal{O}(\varepsilon^2)$ terms exist that have been ignored. Nevertheless, in practice, Eqs. (2.9) can be used for multidimensional problems with space-dependent κ, with the understanding that the resulting solution may not have a strictly $\mathcal{O}(\varepsilon^4)$ error.

2.3. SP_3 Approximation

Now, ignoring terms of $\mathcal{O}(\varepsilon^8)$ in Eq. (2.2), we obtain

$$\begin{aligned} 4\pi B &= \varphi - \frac{\varepsilon^2}{3\kappa^2}\nabla^2\left[\varphi + \frac{4\varepsilon^2}{15\kappa^2}\nabla^2\varphi + \frac{44\varepsilon^4}{315\kappa^4}\nabla^4\varphi\right] + \mathcal{O}(\varepsilon^8) \\ &= \varphi - \frac{\varepsilon^2}{3\kappa^2}\nabla^2\left[\varphi + \left(1 + \frac{11\varepsilon^2}{21\kappa^2}\nabla^2\right)\left(\frac{4\varepsilon^2}{15\kappa^2}\nabla^2\varphi\right)\right] + \mathcal{O}(\varepsilon^8) \\ &= \varphi - \frac{\varepsilon^2}{3\kappa^2}\nabla^2\left[\varphi + \left(1 - \frac{11\varepsilon^2}{21\kappa^2}\nabla^2\right)^{-1}\left(\frac{4\varepsilon^2}{15\kappa^2}\nabla^2\varphi\right)\right] + \mathcal{O}(\varepsilon^8). \end{aligned} \tag{2.10}$$

Hence, if we define

$$\varphi_2 \equiv \left(1 - \frac{11}{21}\frac{\varepsilon^2}{\kappa^2}\nabla^2\right)^{-1}\left(\frac{2\varepsilon^2}{15\kappa^2}\nabla^2\varphi\right), \tag{2.11}$$

then Eq. (2.10) becomes, up to $\mathcal{O}(\varepsilon^8)$,

$$4\pi B = \varphi - \frac{\varepsilon^2}{3\kappa^2}\nabla^2(\varphi + 2\varphi_2),$$

or

$$\forall \nu > \nu_1: \quad -\varepsilon^2 \nabla \cdot \frac{1}{3\kappa}\nabla(\varphi + 2\varphi_2) + \kappa\varphi = \kappa(4\pi B). \tag{2.12a}$$

Equation (2.11) may be written

$$\begin{aligned} -\frac{11\varepsilon^2}{21\kappa^2}\nabla^2\varphi_2 + \varphi_2 = \frac{2}{15}\frac{\varepsilon^2}{\kappa^2}\nabla^2\varphi &= \frac{2}{5}\left(\frac{\varepsilon^2}{3\kappa^2}\nabla^2\varphi\right) \\ &= \frac{2}{5}\left[-4\pi B + \varphi - \frac{2\varepsilon^2}{3\kappa^2}\nabla^2\varphi_2\right], \end{aligned}$$

or

$$\left(\frac{4}{15} - \frac{11}{21}\right)\frac{\varepsilon^2}{\kappa^2}\nabla^2\varphi_2 + \varphi_2 = \frac{2}{5}(\varphi - 4\pi B),$$

or eventually

$$\forall \nu > \nu_1: \quad -\varepsilon^2 \nabla \cdot \frac{9}{35\kappa}\nabla\varphi_2 + \kappa\varphi_2 - \frac{2}{5}\kappa\varphi = -\frac{2}{5}\kappa(4\pi B). \tag{2.12b}$$

By (2.12a), we get up to $\mathcal{O}(\varepsilon^6)$

$$\int_{\nu_1}^{\infty}\int_{S^2} \kappa(B - I)\, d\Omega\, d\nu = -\varepsilon^2 \int_{\nu_1}^{\infty} \nabla \cdot \frac{1}{3\kappa}\nabla(\varphi + 2\varphi_2)\, d\nu.$$

Thus, the energy balance equation (1.4b) becomes

$$\frac{\partial T}{\partial t} = \nabla \cdot k\nabla T + \int_{\nu_1}^{\infty} \nabla \cdot \frac{1}{3\kappa}\nabla(\varphi + 2\varphi_2)\, d\nu. \tag{2.12c}$$

Equation (2.12c) and the two approximate equations (2.12a), (2.12b) form the SP_3 approximation to Eqs. (1.4a) and (1.4b).

The SP_3 equations can be expressed in an algebraically simpler way. Let us calculate $\theta \times \{\text{Eq. (2.12a)}\} + \{\text{Eq. (2.12b)}\}$:

$$-\varepsilon^2 \nabla \cdot \frac{1}{\kappa}\nabla\left\{\frac{\theta}{3}(\varphi + 2\varphi_2) + \frac{9}{35}\varphi_2\right\} + \kappa\left\{\theta\varphi + \varphi_2 - \frac{2}{5}\varphi\right\} = \kappa\left(\theta - \frac{2}{5}\right)(4\pi B).$$

We seek values of θ such that the two functions in the braces on the left are scalar multiples of each other. More explicitly, we look for values of θ such that

$$\frac{\theta}{3}(\varphi + 2\varphi_2) + \frac{9}{35}\varphi_2 = \mu^2\left(\theta\varphi + \varphi_2 - \frac{2}{5}\varphi\right), \tag{2.13}$$

where $\mu^2 > 0$ is a constant to be determined. Equation (2.13) holds for arbitrary φ and φ_2 iff

$$\frac{\theta}{3} = \mu^2\left(\theta - \frac{2}{5}\right) \quad \text{and} \quad \frac{2\theta}{3} + \frac{9}{35} = \mu^2.$$

Eliminating θ, we obtain a quadratic equation in μ^2,

$$\frac{1}{2}\mu^2 - \frac{9}{70} = \mu^2\left(\frac{2}{3}\mu^2 - \frac{11}{14}\right),$$

which has two positive real solutions,

$$\mu_1^2 = \frac{3}{7} - \frac{2}{7}\sqrt{\frac{6}{5}} \quad \text{and} \quad \mu_2^2 = \frac{3}{7} + \frac{2}{7}\sqrt{\frac{6}{5}}.$$

The corresponding values of θ are

$$\theta_1 = \frac{9}{35} - \frac{3}{7}\sqrt{\frac{6}{5}} \quad \text{and} \quad \theta_2 = \frac{9}{35} + \frac{3}{7}\sqrt{\frac{6}{5}}.$$

Now, relation (2.13) implies, for $n = 1, 2$,

$$\left(-\nabla \cdot \frac{\varepsilon^2\mu_n^2}{\kappa}\nabla + \kappa\right)\left[\theta_n\varphi + \varphi_2 - \frac{2}{5}\varphi\right] = \left(\theta_n - \frac{2}{5}\right)\kappa(4\pi B). \tag{2.14}$$

This suggests that we define two new independent variables for $n = 1, 2$,

$$\psi_n = \frac{\theta_n\varphi + \varphi_2 - 2/5\varphi}{\theta_n - 2/5} = \varphi + \frac{1}{\theta_n - 2/5}\varphi_2 = \varphi + \gamma_n\varphi_2, \tag{2.15}$$

where

$$\gamma_n = \frac{1}{\theta_n - 2/5} = \frac{5}{7}\left[1 + (-1)^n 3\sqrt{\frac{6}{5}}\right].$$

The two equations in (2.14) become

$$-\nabla \cdot \frac{\varepsilon^2\mu_1^2}{\kappa}\nabla\psi_1 + \kappa\psi_1 = \kappa(4\pi B), \tag{2.16a}$$

$$-\nabla \cdot \frac{\varepsilon^2\mu_2^2}{\kappa}\nabla\psi_2 + \kappa\psi_2 = \kappa(4\pi B). \tag{2.16b}$$

The advantage of this form of the SP_3 equations is that the diffusion equations are uncoupled. However, we show below in section 3 that a weak coupling remains in the boundary conditions.

The linear transformation of variables above is inverted according to the formulae

$$\varphi = \frac{\gamma_2\psi_1 - \gamma_1\psi_2}{\gamma_2 - \gamma_1} \quad \text{and} \quad \varphi_2 = \frac{\psi_2 - \psi_1}{\gamma_2 - \gamma_1}. \tag{2.17}$$

Defining three constants

$$w_0 = \frac{1}{\gamma_2 - \gamma_1} = \frac{7}{30}\sqrt{\frac{5}{6}} = \frac{7}{36}\sqrt{\frac{6}{5}}, \tag{2.18a}$$

$$w_1 = \frac{\gamma_2}{\gamma_2 - \gamma_1} = \frac{1}{6}\left(3 + \sqrt{\frac{5}{6}}\right), \quad w_2 = \frac{-\gamma_1}{\gamma_2 - \gamma_1} = \frac{1}{6}\left(3 - \sqrt{\frac{5}{6}}\right), \tag{2.18b}$$

we can write $\varphi = w_1\psi_1 + w_2\psi_2$ and $\varphi_2 = w_0(\psi_2 - \psi_1)$, and we have furthermore

$$\frac{1}{3}(\varphi + 2\varphi_2) = \frac{1}{3}(w_1 - 2w_0)\psi_1 + \frac{1}{3}(w_2 + 2w_0)\psi_2 = a_1\psi_1 + a_2\psi_2.$$

Here again we have introduced constants

$$a_1 = \frac{w_1 - 2w_0}{3} = \frac{1}{30}\left(5 - 3\sqrt{\frac{5}{6}}\right), \quad a_2 = \frac{w_2 + 2w_0}{3} = \frac{1}{30}\left(5 + 3\sqrt{\frac{5}{6}}\right).$$

In this way, the SP_3 energy balance equation (2.12c) above becomes

$$\frac{\partial T}{\partial t} = \nabla \cdot k\nabla T + \int_{\nu_1}^{\infty} \nabla \cdot \frac{1}{\kappa}\nabla(a_1\psi_1 + a_2\psi_2)\, d\nu. \tag{2.19}$$

Thus, the SP_3 equations can also be written as Eqs. (2.16) and (2.19). As before, these equations are strictly asymptotic only if κ is independent of space, or if the entire problem has planar-geometry space dependence.

For general multidimensional problems, it is easily seen that the SP_1 and P_1 equations are identical. Also, for planar geometry, the SP_N and respective P_N equations are identical for all N. However, for general multidimensional problems, and for all $N \geq 2$, the SP_N equations are fewer in number and simpler in structure than the corresponding P_N equations.

3. SP_N BOUNDARY CONDITIONS

In the previous section, we used a formal asymptotic analysis in the interior of the glass system to derive the SP_N approximations to the radiative transfer equations. To obtain boundary conditions for the SP_N equations, a traditional asymptotic approach would employ a boundary layer analysis on the outer boundary of the system. Unfortunately, this approach is impractical because of the extreme complexity of the (asymptotically) high-order terms that would have to be included. Thus, to obtain boundary conditions for use in practical applications, we follow a simpler (non-asymptotic) approach.

This same difficulty occurs in the field of neutron transport—the asymptotic derivation of the SP_N equations is relatively straightforward, but the asymptotic derivation of boundary conditions for these equations is extremely complicated. However, the steady-state neutron transport SP_N equations themselves, and corresponding boundary conditions, can be also derived from a variational principle; see [1, 15]. The variational analysis is extremely lengthy, but the results are fairly simple and in practice work well (i.e., are accurate). Here, we use the boundary conditions developed for neutron transport to state (and rewrite in a more suitable form) the boundary conditions for the SP_1, SP_2, and SP_3 approximations to the transport problem (1.4b) with the boundary condition (1.1c). Later, in the Discussion (Section 4), we describe a formal procedure by which the multidimensional SP_N equations and boundary conditions stated below can be obtained from the planar-geometry P_N equations and boundary conditions.

We consider the transport equation (1.4b)

$$\forall \nu > \nu_1: \quad \varepsilon\Omega \cdot \nabla I(x, \Omega) + \kappa I(x, \Omega) = \kappa B, \quad x \in V,$$

with semi-transparent boundary conditions on ∂V

$$I(x, \Omega) = \rho(n \cdot \Omega) I(x, \Omega') + [1 - \rho(n \cdot \Omega)] B(\nu, T_b), \quad n \cdot \Omega < 0.$$

As before, we define the following quantity (which in common notation is $4\pi \times$ the mean intensity):

$$\varphi(x) = \int_{S^2} I(x, \Omega)\, d\Omega.$$

We also define two integrals of the penetrating radiation [see Eq. (1.2a)]: for $m = 1$ and 3,

$$\begin{aligned} I_m(x, \nu) &= \int_{n \cdot \Omega < 0} P_m(|\Omega \cdot n|) I_p(\Omega, \nu)\, d\Omega \\ &= \left(\int_{n \cdot \Omega < 0} P_m(|\Omega \cdot n|)[1 - \rho(n \cdot \Omega)]\, d\Omega \right) B(\nu, T_b) \\ &= \left(2\pi \int_0^1 P_m(\mu)[1 - \rho(-\mu)]\, d\mu \right) B(\nu, T_b) \\ &= \rho_m B(\nu, T_b), \end{aligned} \tag{3.1a}$$

where

$$\rho_m = \begin{cases} (1 - 2r_1)\pi, & m = 1, \\ -\left(\dfrac{1}{4} + 2r_5 \right)\pi, & m = 3. \end{cases} \tag{3.1b}$$

Here, we have used the Legendre polynomials of order 1 and 3,

$$P_1(\mu) = \mu \quad \text{and} \quad P_3(\mu) = \frac{5}{2}\mu^3 - \frac{3}{2}\mu,$$

and we have defined the integrals:

$$\begin{aligned} r_1 &= \int_0^1 \mu \rho(-\mu)\, d\mu, & r_5 &= \int_0^1 P_3(\mu) \rho(-\mu)\, d\mu, \\ r_2 &= \int_0^1 \mu^2 \rho(-\mu)\, d\mu, & r_6 &= \int_0^1 P_2(\mu) P_3(\mu) \rho(-\mu)\, d\mu, \\ r_3 &= \int_0^1 \mu^3 \rho(-\mu)\, d\mu, & r_7 &= \int_0^1 P_3(\mu) P_3(\mu) \rho(-\mu)\, d\mu. \\ r_4 &= \int_0^1 \mu P_3(\mu) \rho(-\mu)\, d\mu, \end{aligned}$$

The boundary conditions in [1, 15] were derived for the case $\rho = 0$. For semi-transparent boundary conditions, the same arguments apply and the calculations can be analogously carried out, the only difference being modifications in the coefficients. We therefore content ourselves with stating the results.

In the SP_1 approximation (2.3a), the boundary condition for φ is

$$\forall \nu > \nu_1: \quad \varphi(x) + \left(\frac{1+3r_2}{1-2r_1}\frac{2\varepsilon}{3\kappa}\right) n \cdot \nabla\varphi(x) = 4\pi B_b(x), \tag{3.2}$$

where $B_b(x) = B(\nu, T_b(x))$.

In the SP_2 approximation (2.9b), the boundary condition for φ is [15]

$$\begin{aligned}\varphi(x) + \left(\frac{1+3r_2}{1-2r_1}\frac{2\varepsilon}{3\kappa}\right) n \cdot \nabla\left(\varphi(x) + \frac{4}{5}[\varphi(x) - 4\pi B(x)]\right) \\ + \left(\frac{1-12r_3+4r_1}{2(1-2r_1)}\right)[\varphi(x) - 4\pi B(x)] = 4\pi B_b(x),\end{aligned} \tag{3.3}$$

where $B(x) = B(\nu, T(x))$. We note that Eq. (3.3) reduces to Eq. (3.2) if we delete the $[\varphi - 4\pi B]$ terms. Equation (3.3) can be written by using Eq. (2.8) as

$$\varphi = \frac{5}{9}\xi + \frac{4}{9}(4\pi B)$$

to replace φ by the SP_2 dependent variable ξ. We obtain, after straightforward algebra,

$$\begin{aligned}\forall \nu > \nu_1: \quad \xi(x) + \left(\frac{1+3r_2}{1-4r_3}\frac{4\varepsilon}{5\kappa}\right) n \cdot \nabla\xi(x) \\ = 4\pi B(x) + \left(\frac{1-2r_1}{1-4r_3}\frac{6}{5}\right)[4\pi B_b(x) - 4\pi B(x)].\end{aligned} \tag{3.4}$$

Finally, the SP_3 boundary conditions for φ and φ_2 in (2.12a) and (2.12b) are [1]: for all frequencies $\nu > \nu_1$ and $x \in \partial V$,

$$\begin{aligned}(1-2r_1)\frac{1}{4}\varphi(x) + (1-8r_3)\frac{5}{16}\varphi_2(x) + (1+3r_2)\frac{\varepsilon}{6\kappa} n \cdot \nabla\varphi(x) \\ + \left(\frac{1+3r_2}{3} + \frac{3r_4}{2}\right)\frac{2\varepsilon}{3\kappa} n \cdot \nabla\varphi_2(x) = \rho_1 B_b(x),\end{aligned} \tag{3.5a}$$

$$\begin{aligned}-(1+8r_5)\frac{1}{16}\varphi(x) + (1-8r_6)\frac{5}{16}\varphi_2(x) + 3r_4\frac{\varepsilon}{6\kappa} n \cdot \nabla\varphi(x) \\ + \left(r_4 + \frac{3}{14}(1+7r_7)\right)\frac{\varepsilon}{\kappa} n \cdot \nabla\varphi_2(x) = \rho_3 B_b(x),\end{aligned} \tag{3.5b}$$

or formally

$$\begin{aligned}A_1\varphi(x) + A_2\varphi_2(x) + A_3\frac{\varepsilon}{\kappa} n \cdot \nabla\varphi(x) + A_4\frac{\varepsilon}{\kappa} n \cdot \nabla\varphi_2(x) = \rho_1 B_b(x), \\ B_1\varphi(x) + B_2\varphi_2(x) + B_3\frac{\varepsilon}{\kappa} n \cdot \nabla\varphi(x) + B_4\frac{\varepsilon}{\kappa} n \cdot \nabla\varphi_2(x) = \rho_3 B_b(x).\end{aligned}$$

Using the formulae in Eq. (2.17), we can transform the above boundary conditions for φ

and φ_2 into boundary conditions for ψ_1 and ψ_2. We obtain

$$\begin{aligned}
&w_0(\gamma_2 A_1 - A_2)\psi_1 + w_0(A_2 - \gamma_1 A_1)\psi_2 + w_0(\gamma_2 A_3 - A_4)\frac{\varepsilon}{\kappa} n \cdot \nabla\psi_1 \\
&\quad + w_0(A_4 - \gamma_1 A_3)\frac{\varepsilon}{\kappa} n \cdot \nabla\psi_2 = \rho_1 B_b, \\
&w_0(\gamma_2 B_1 - B_2)\psi_1 + w_0(B_2 - \gamma_1 B_1)\psi_2 + w_0(\gamma_2 B_3 - B_4)\frac{\varepsilon}{\kappa} n \cdot \nabla\psi_1 \\
&\quad + w_0(B_4 - \gamma_1 B_3)\frac{\varepsilon}{\kappa} n \cdot \nabla\psi_2 = \rho_3 B_b,
\end{aligned}$$

or again, formally rewritten for convenience,

$$\begin{aligned}
C_1\psi_1 + C_2\psi_2 + C_3\frac{\varepsilon}{\kappa} n \cdot \nabla\psi_1 + C_4\frac{\varepsilon}{\kappa} n \cdot \nabla\psi_2 = \rho_1 B_b, \\
D_1\psi + D_2\psi_2 + D_3\frac{\varepsilon}{\kappa} n \cdot \nabla\psi_1 + D_4\frac{\varepsilon}{\kappa} n \cdot \nabla\psi_2 = \rho_3 B_b.
\end{aligned}$$

We eliminate the gradient term $n \cdot \nabla\psi_2$ in the first equation and $n \cdot \nabla\psi_1$ in the second to get boundary conditions for the ψ_1 and ψ_2 equations, respectively. We find

$$\begin{aligned}
&(C_1 D_4 - D_1 C_4)\psi_1 + (C_3 D_4 - D_3 C_4)\frac{\varepsilon}{\kappa} n \cdot \nabla\psi_1 \\
&\quad = -(C_2 D_4 - D_2 C_4)\psi_2 + (D_4\rho_1 - C_4\rho_3)B_b, \\
&-(C_2 D_3 - D_2 C_3)\psi_2 + (C_3 D_4 - D_3 C_4)\frac{\varepsilon}{\kappa} n \cdot \nabla\psi_2 \\
&\quad = (C_1 D_3 - D_1 C_3)\psi_1 - (D_3\rho_1 - C_3\rho_3)B_b.
\end{aligned}$$

Thus, if we set $D = C_3 D_4 - D_3 C_4$ and define constants

$$\begin{aligned}
\alpha_1 &= \frac{C_1 D_4 - D_1 C_4}{D}, \quad \alpha_2 = \frac{C_3 D_2 - C_2 D_3}{D}, \\
\beta_1 &= \frac{C_3 D_1 - D_3 C_1}{D}, \quad \beta_2 = \frac{C_2 D_4 - D_2 C_4}{D}, \\
\eta_1 &= \frac{D_4\rho_1 - C_4\rho_3}{D}, \quad \eta_2 = \frac{C_3\rho_3 - D_3\rho_1}{D},
\end{aligned}$$

we obtain the following SP_3 boundary conditions:

$$\alpha_1\psi_1(x) + \frac{\varepsilon}{\kappa} n \cdot \nabla\psi_1(x) = -\beta_2\psi_2(x) + \eta_1 B_b, \tag{3.6a}$$

$$\alpha_2\psi_2(x) + \frac{\varepsilon}{\kappa} n \cdot \nabla\psi_2(x) = -\beta_1\psi_1(x) + \eta_2 B_b. \tag{3.6b}$$

Equations (3.6a) and (3.6b) go with the diffusion equations (2.16a) and (2.16b), respectively. The coupling of ψ_1 and ψ_2 in the above boundary conditions is weak.

As an example, let us consider the simple case of no reflection ($\rho = 0$). Then, the constants $r_1, \ldots, r_7$ are all zero. We find after some calculations that $D = \frac{1}{144}\sqrt{6/5}$, and the constants

in Eqs. (3.6) are

$$\alpha_1 = \frac{5}{96}\left(34 + 11\sqrt{\frac{6}{5}}\right), \quad \alpha_2 = \frac{5}{96}\left(34 - 11\sqrt{\frac{6}{5}}\right),$$
$$\beta_1 = \frac{5}{96}\left(2 - \sqrt{\frac{6}{5}}\right), \qquad \beta_2 = \frac{5}{96}\left(2 + \sqrt{\frac{6}{5}}\right),$$
$$\eta_1 = \frac{5\pi}{2}\left(3 + \sqrt{\frac{6}{5}}\right), \qquad \eta_2 = \frac{5\pi}{2}\left(3 - \sqrt{\frac{6}{5}}\right).$$

We note that $0 < \beta_n \ll \alpha_n$. Thus, the simple strategy of solving the two diffusion problems independently (within a single iteration) and iterating on the coefficients of β_n will converge rapidly.

The boundary conditions described above were obtained from a variational analysis, not from an asymptotic boundary layer analysis. They should be accurate because the exterior incident flux is isotropic, i.e. is a smooth function of μ. These boundary conditions hold for general multidimensional sytems having a smooth outer surface with outer normal n.

For the special cases of (i) the SP_1 equations in general geometry, and (ii) the general SP_N equations in planar geometry, the above boundary conditions reduce to the *Marshak* boundary conditions, which are well-known in neutron transport. Also, in these two respective cases, we have seen that (i) the SP_1 and P_1 equations are identical, and (ii) the SP_N and P_N equations are identical. Therefore: (i) in general geometry, the SP_1 equations and boundary conditions are identical to the P_1 equations and boundary conditions, and (ii) in planar geometry, and for general N, the SP_N equations and boundary conditions are identical to the P_N equations and boundary conditions. For non-planar geometry and $N \geq 2$, the SP_N and P_N approximations differ.

4. NUMERICAL SOLUTIONS OF 1-D PROBLEMS

Here we investigate numerical simulations for one-dimensional slab geometry. We used a standard finite difference technique to discretize the diffusion equations, with uniform space and time grids. We chose a grid size 0.01 for the scaled interval [0, 1] and the time step 0.0001. We assumed the scaled physical parameters k and h in the equations to have the values $k = 1$ and $h = 1$. The edge of the opaque part of the spectrum was located at the wavelength $\lambda_1 = 7$ μm, thus giving $\nu_1 = c/\lambda_1 = 4.28 \cdot 10^{13}\ \mathrm{s}^{-1}$. The refractive coefficients were chosen to be $n_1 = 1.46$ and $n_2 = 1$ for glass and air, respectively. Hence, the corresponding hemispheric emissivity was $\alpha = 0.92$. Typical values of the physical constants for glass are used: $c_m = 900$ W/kg K, $\rho_m = 2200\ \mathrm{kg/m}^3$. We simulated the annealing of a glass slab surrounded by air at room temperature $T_b = 300$ K. The outside radiation was assumed to be Planckian with temperature T_b. The calculation started with the constant initial temperature $T_0(x) = 1000$ K.

Different optical regimes were considered, corresponding to different values of the non-dimensional parameter ε. Since the SP_N approximations were derived asymptotically for $\varepsilon \ll 1$ the results should agree well with the full transport solution when ε is small, i.e., in the optically thick regime.

Figure 1 shows the three SP_N approximations in comparison to the radiative transfer solution and the Rosseland approximation at time $t = 0.01$, using a single frequency band,

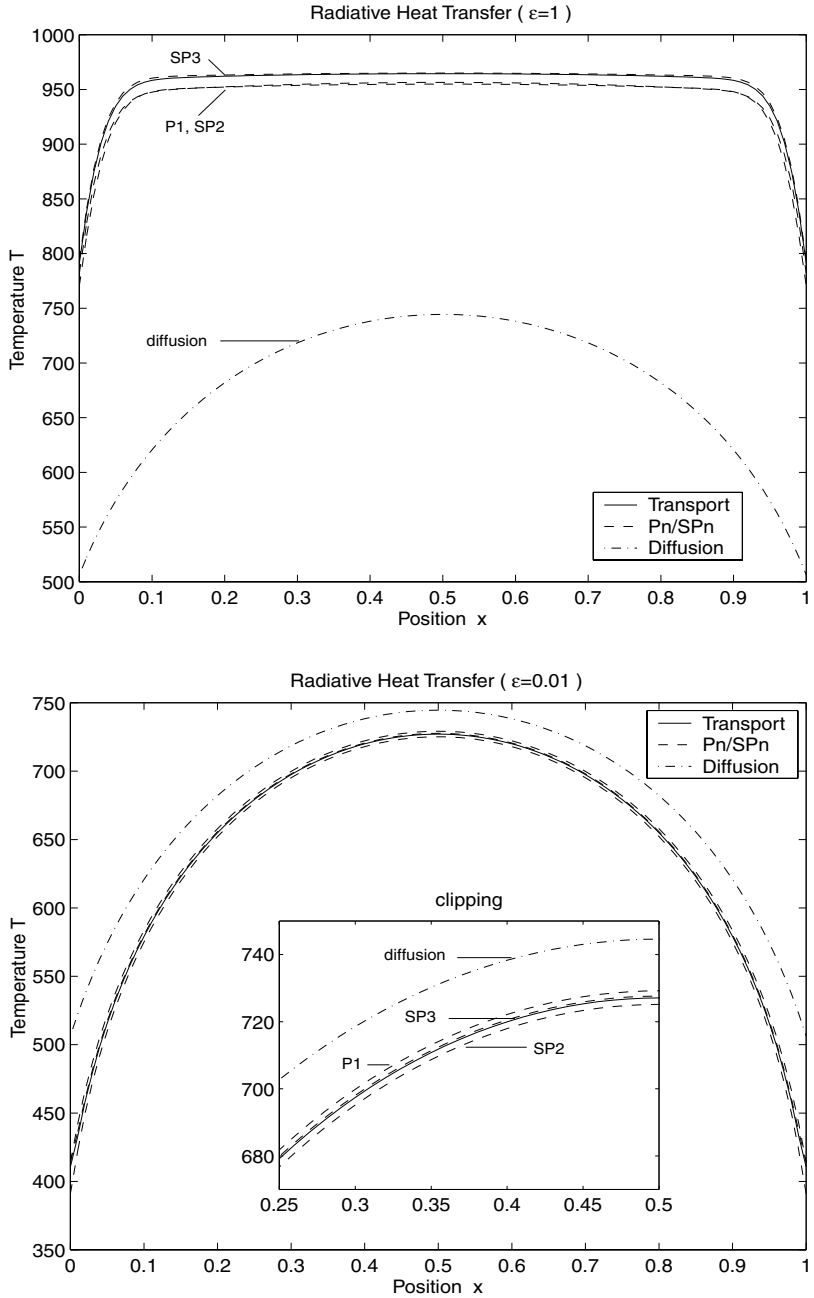

FIG. 1. Comparison of the diffusion and SP_N approximations for one frequency band. Results are shown for the intermediate regime ($\varepsilon = 1$, top) and the optically thick, diffusive regime ($\varepsilon = 0.01$, bottom).

and with $\varepsilon = 1$ and $\varepsilon = 0.01$ respectively. As can be observed, the above approximations, in particular the SP_3 approximation, yield much better results than the conventional equilibrium diffusion approximation. In particular, in the intermediate regime with $\varepsilon = 1$ they perform quite well, although the asymptotics would not suggest this. [The reason might be that the SP_1, SP_2, and SP_3 approximations can be derived in a different way using variational

TABLE I
Computational Costs of the Different Approximations and the Full Transport Model in the 1-D Problem Above

	Ross.	SP_1	SP_2	SP_3	RHT
Flops ($\times 10^6$)	8.2	14.3	14.3	26.9	490.0
Time (s)	21.0	30.0	30.3	42.2	812.8

methods [1, 8, 15]. Using this approach, one finds that the SP_N approximations are accurate if the radiation field is relatively isotropic, which is true in our case.] Furthermore, the SP_N approximations become more accurate the smaller ε is—i.e., the more optically thick and diffusive the regime is—as we expect from the asymptotic analysis.

A comparison of the run times of the different algorithms reveals that the SP_1 and SP_2 calculations took roughly 1.5 times (and the SP_3 calculation took approximately 2.0 times) the computational effort to solve the classical Rosseland equation (Table I; data measured on a PC with AMD-K6 200 processor running MATLAB 5 under Linux 2.2). Nevertheless, the SP_N approximations were solved *much* faster than the full radiative transfer problem.

We also considered a discontinuity in the opacity κ, corresponding to two different materials in the left and right halves of the slab. Figure 2 shows the computed numerical solutions for two different magnitudes of the jump. In both simulations, $\varepsilon = 0.1$. Again, the SP_N approximations give much more accurate results than the classical diffusion approximation. We remark that the asymptotic considerations were performed for absorption coefficients κ which are independent of space. The SP_N equations are not strictly asymptotic in the general situation of a multidimensional problem with space-dependent κ. However, in the special case of planar geometry with spatially-varying κ, the SP_N equations are still asymptotically valid.

5. NUMERICAL SOLUTIONS OF MULTI-D PROBLEMS

It is particularly important to investigate multidimensional geometries because for $N \geq 2$, the SP_N and P_N equations are equivalent in 1-D, but not in 2-D or 3-D.

We investigate different absorption rates κ as functions of the frequency ν. First, we consider a situation with only one frequency band, i.e., a constant absorption rate $\kappa = 1$ on the non-opaque interval (ν_1, ∞). Second, we consider a case more relevant for the simulation of glass cooling with the following eight frequency bands: $[\nu_i, \nu_{i+1}]$, $i = 1, \ldots, 8$ with piecewise constant absorption rate $\kappa(\nu) = \kappa_i$, $\nu \in [\nu_i, \nu_{i+1}]$ (Table II).

Now, we consider a 2-D circle with radius $r = 0.5$. We use an equidistant step size $\Delta r = 0.005$ and calculate the solution at time $t = 0.001$. Except for the opacity κ, we used the same parameter set as in the 1-D case. In particular, we used $\varepsilon = 1$ and $k = 1$. In Fig. 3, the transport solution is plotted, together with the SP_N approximations and the Rosseland approximation. This figure reveals that again the SP_N approximations—in particular, SP_3 — coincide very well with the transport solution.

Finally, we treated a 3-D problem with the eight frequency bands defined above. We simulate the cooling of a glass cube of side length 1.0 cm, with a uniform initial temperature distribution $T_0 = 900$ K and outside temperature $T_b = 293.15$ K. The dimensionless parameter ε had the fixed value 1, and we set $k = 100$, while the remaining parameters were the same as in the previous examples.

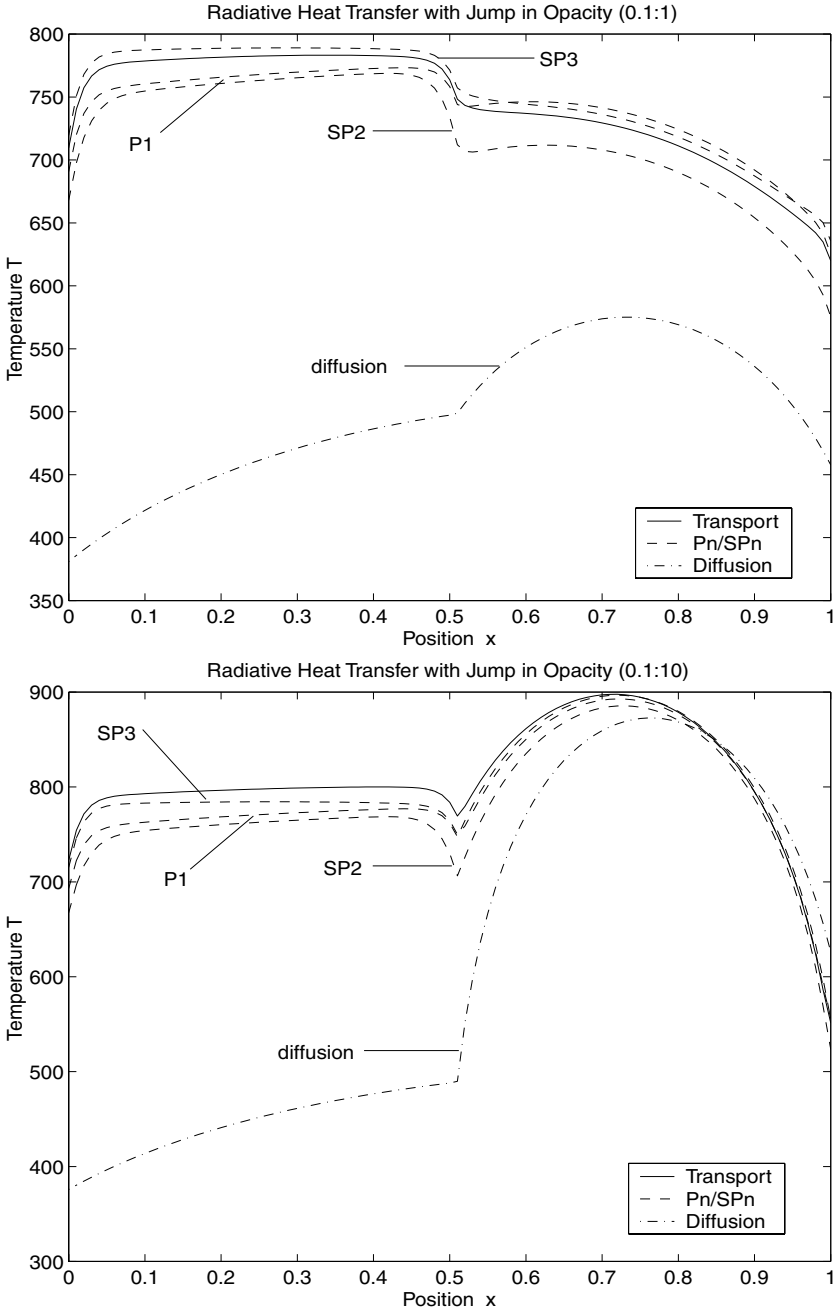

FIG. 2. Temperatures in the presence of discontinuous opacities. The top figure corresponds to $\kappa = 0.1$ in the left half of the slab and $\kappa = 1$ in the right half; the bottom figure corresponds to $\kappa = 0.1$ in the left half of the slab and $\kappa = 10$ in the right half.

Figure 4 shows a comparison of the SP_N solutions and the full transport solution, and Fig. 5 displays the exact 3-D temperature distribution in the cube, at time $t = 0.01$. For the simulation of the full transport model in three dimensions, we employed a ray tracing algorithm implemented by one of the authors. A grid spacing of 21 points per space direction

TABLE II
Absorption Cross Sections of an Eight-Band Model for Glass

Band i	λ_i [μm]	λ_{i+1} [μm]	κ_i [1/m]
1	0	0.20	0.40
2	0.20	3.00	0.50
3	3.00	3.50	7.70
4	3.50	4.00	15.45
5	4.00	4.50	27.98
6	4.50	5.50	267.98
7	5.50	6.00	567.32
8	6.00	7.00	7136.06
—	7.00	∞	opaque

Note. The bands are defined by wavelength intervals (data kindly provided by ITWM, Kaiserslautern).

was used. The SP_N approximations were checked against the results of this method. It can be seen that they match the temperature of the latter very well, and are much more accurate than standard equilibrium diffusion. In particular, they reconstruct the temperature near the boundary much more faithfully than Rossland's approximation. This is due to the fact that the Rosseland model does not include boundary layer effects, while SP_1 and the higher order approximations do so. Good agreement of the temperature distribution at the boundary is also observed in the 1-D and 2-D cases considered above.

In each of the above simulations, the SP_N solutions exhibit physically correct boundary layers that are not present in the Rosseland solution. This raises an important computational

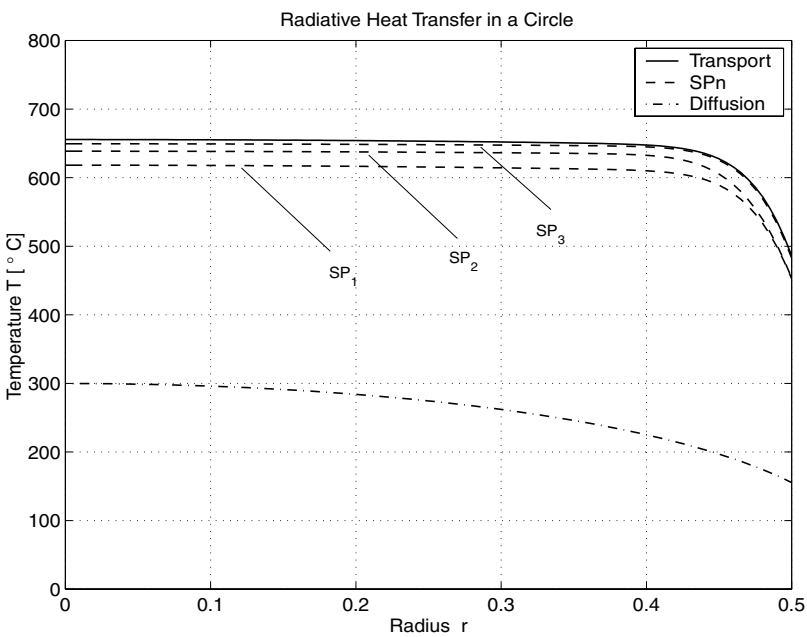

FIG. 3. Radial temperature distribution in a 2-D circle at time $t = 0.001$ using the eight-band model for the frequency dependence of the the opacity with piecewise constant $\kappa(\nu)$.

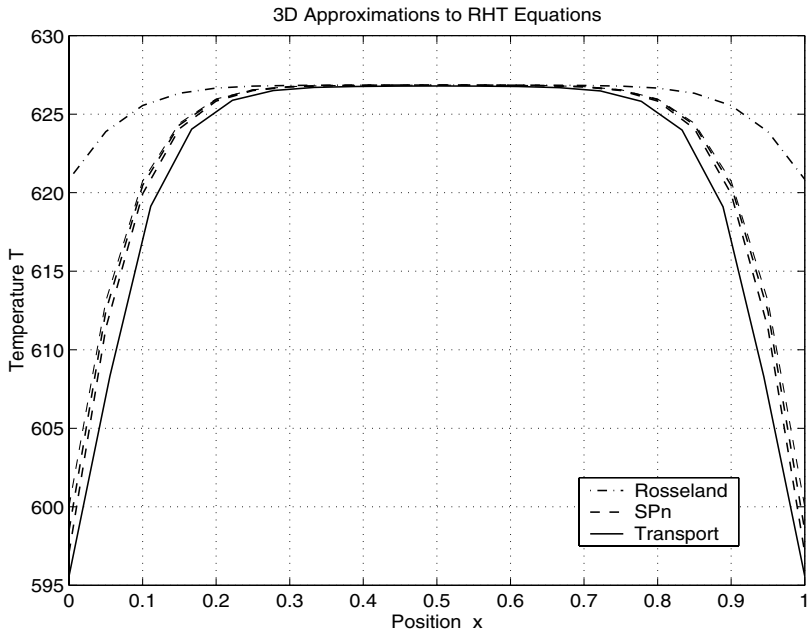

FIG. 4. Temperature along a line passing through the center of the 3-D cube at time $t = 0.01$.

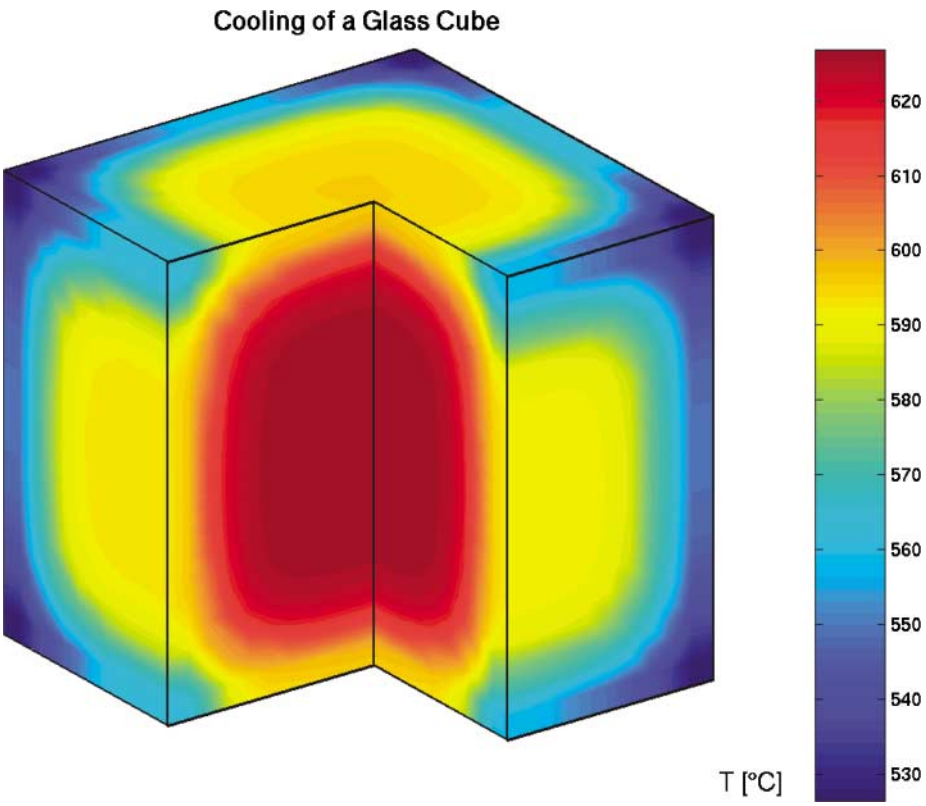

FIG. 5. 3-D temperature distribution in the cube.

issue: to accurately capture these boundary layers numerically, the discrete SP_N equations must be solved on a finer spatial grid than is required for the Rosseland equation. Thus, to achieve an accurate description of temperature boundary layers in the annealing of glass, it is necessary to (i) employ a more sophisticated theory than the Rosseland approximation, and (ii) use a finer spatial grid, at least in the boundary-layer regions where large temperature derivatives occur.

Finally, we comment that in 2-D and 3-D problems, the cost of the SP_N calculations compared to the cost of the full radiative transfer calculation is *less* than in 1-D. There are at least two reasons for this. First, the mathematical theory for obtaining efficient numerical solutions of diffusion equations is much more mature than the corresponding theory for solving multidimensional tranport problems. (For example, multigrid methods are generally available for diffusion calculations, but not for transport calculations.) Second, in going from 1-D to 2-D, the number of independent variables in diffusion problems increases by one (one spatial variable), while the number of independent variables in transport problems increases by *two* (one spatial variable and one angular variable).

6. DISCUSSION

We have developed asymptotic approximations—the so-called SP_N equations—to the equations of radiative heat transfer in glass, for problems that are optically thick and diffusive. The simplest such approximation is equilibrium diffusion theory, which itself is an approximation to the SP_1 equations. Formally, and under ideal circumstances, the SP_N approximations for increasing N are increasingly higher-order asymptotic approximations to the radiative transfer equations. However, two non-asymptotic approximations may interfere with the strictness of this asymptotic pedigree: a space-dependent value of κ, and the use of variationally derived boundary conditions.

In multidimensional geometries with $N \geq 2$, the SP_N equations are a considerably smaller and less complicated set of equations than the standard spherical harmonic (P_N) equations. In the field of neutron transport, the SP_N equations have been tested fairly extensively, and have been shown to be a significant, robust, and relatively inexpensive way to improve the accuracy of classic diffusion theory. We believe that these advantages apply as well for radiative transfer in glass.

A numerical investigation of the above SP_N equations shows that the conjecture in the above paragraph is correct. Specifically, we have shown that (i) the SP_N equations are accurate approximations to the radiative heat transfer equations, even when the regime becomes less diffusive, and (ii) the complexity and cost of solving the SP_N equations is considerably reduced in comparison to the full radiative heat transfer problem.

The SP_N theories developed in the present paper are based on the assumption that a mean free path is small compared to the distance over which the solution varies by an $\mathcal{O}(1)$ amount. This is generally true only if the glass object that is cooling down is convex. If the glass object is not convex, then a significant number of photons that leak out of the exterior surface will *stream* through the surrounding air (where the mean free path is long) and then re-enter V at some relatively distant point on ∂V. To model this phenomenon correctly, the transport process must be simulated outside V, at least for the part of the exterior of V through which exiting photons stream en route to re-entering V at another boundary point. Unfortunately, the SP_N approximation is generally inaccurate in the exterior of V, where

the mean free paths are not small. Hence, the SP_N (and Rosseland) theories are generally accurate only for convex domains.

We now make some general observations on the mathematical analysis and the results developed in this paper. The analysis used to derive the SP_N equations is clearly asymptotic in nature, using the *diffusive* scaling contained in Eqs. (1.4), together with the assumptions that (i) $\varepsilon \ll 1$ and (ii) the solution and its spatial derivatives are $\mathcal{O}(1)$ in magnitude.

Our first comment is that in this paper, we do not derive an expansion of the *solution* of the underlying radiative transfer problem. Instead, we obtain an expansion of the transport *operator*. Our first result is the (infinitely) high-order differential equation (2.2), from which we derive the second-order SP_1, SP_2, and SP_3 equations. Thus, for us, the term "higher-order approximations" does not mean that we have expanded the solution and calculated the coefficients (of the solution) for increasingly higher powers of ε. Rather, we have calculated robust and increasingly more accurate (systems of) equations, from which a more accurate solution can be obtained numerically.

Second, as already mentioned, the first result of our asymptotic analysis is Eq. (2.2): a differential equation of *infinitely high order*. However, we *do not* recommend that this equation, or approximations to it obtained just by deleting terms equal to or smaller than $\mathcal{O}(\varepsilon^4)$, be solved directly. We *do* recommend that asymptotic (SP_N) aproximations to Eq. (2.2), having the form of coupled systems of second-order elliptic (diffusion) equations, be solved instead. These coupled diffusion equations are asymptotically equivalent to Eq. (2.2), but they are robust and easier to solve computationally. To put this another way, we recommend that coupled systems of second-order differential equations be solved, rather than one higher (fourth, or sixth, etc.)-order differential equation.

Third, the multidimensional SP_N equations and boundary conditions derived in this paper reduce, for the special case of planar geometry, to the familiar planar-geometry P_N equations and Marshak boundary conditions. A simple but formal procedure to derive the multidimensional SP_N equations and boundary conditions from the planar-geometry P_N equations and boundary conditions is as follows:

1. For planar geometry radiative transfer problems, derive the familiar planar-geometry P_N equations and boundary conditions. (These are a coupled system of first-order equations, which are differential in the spatial variable.)
2. Algebraically eliminate the odd-order angular moments from the equations derived in step 1. (This produces a coupled system of second-order differential equations and boundary conditions.)
3. In the system of second-order differential equations from step 2, formally replace the 1-D Laplacian operator by the multi-D Laplacian operator,

$$\frac{d}{dx}D(x)\frac{d}{dx} \quad \text{by } \nabla \cdot D(x, y, z)\nabla, \tag{6.1}$$

and in the boundary conditions from step 2, formally replace

$$\pm\frac{d}{dx} \quad \text{by } n \cdot \nabla \tag{6.2}$$

where $+$ or $-$ is chosen so that the *outer* derivative on the boundary is obtained.

It is obvious that the multidimensional SP_N equations obtained in step 3 reduce to the second-order P_N equations for the special case of planar geometry.

For many years, this formal procedure was the only known way to derive the neutron transport SP_N equations and boundary conditions from the linear Boltzmann equation. This perceived weakness in the theoretical foundation of the SP_N approximations resulted in the lack of acceptance of these approximations in the nuclear reactor community, even though numerical simulations, sporadically obtained over many years, showed that the SP_N solutions with $N > 2$ are consistently more accurate than the P_1 solutions. However, in the previous decade, more rigorous asymptotic and variational methods have been used to achieve the derivations of the neutron transport SP_N equations and boundary conditions [1, 8]. Generalizations of those approaches are presented in this paper for radiative heat transfer in glass.

Fourth, the asymptotic expansion used in this paper assumes that the solution and its spatial derivatives are $\mathcal{O}(1)$. Thus, this expansion seems *not* to be one that should lead to accurate descriptions of spatial boundary layers, where spatial derivatives are $\mathcal{O}(\varepsilon^{-1})$. Nevertheless, our numerical results show that the SP_N approximations are *much* more accurate than the Rosseland approximation in the boundary layer regions. It is not obvious to us why this happens, but experimentally, it does. There may be theoretical principles at work here that we do not yet fully understand.

In the field of nonlinear gas dynamics, governed by the nonlinear Boltzmann equation, a situation occurs which is quite similar to the one seen in this paper: an asymptotic expansion (related to the one employed here) leads to the second-order Navier–Stokes equations, with the (higher-order) Burnett equations arising as higher-order (in ε) asymptotic corrections. [The Navier–Stokes equations correspond to Eq. (2.2) with $\mathcal{O}(\varepsilon^4)$ terms discarded; the Burnett equations correspond to Eq. (2.2) with $\mathcal{O}(\varepsilon^n)$ terms discarded, with $n \geq 6$.] The Burnett equations themselves have not been generally successful in producing accurate transport corrections to the Navier–Stokes equations [2]. However, a restructuring of these equations into, for example, asymptotically equivalent coupled systems of second-order differential equations might be advantageous—if this is algebraically feasible. Such a stragegy is clearly advantageous for neutron transport [1, 8]; it has recently been shown to be advantageous in the derivation of more accurate Fokker–Planck approximations for electron transport [10], and we show in this paper that it is advantageous for radiative heat transfer in glass. This strategy might be beneficial for other particle transport problems as well.

It is appropriate to comment on the physical assumption in this paper that ε, the ratio of a typical mean free path to a typical length scale of the solution (say, a typical diameter of the system) is small. This assumption is definitely *not* valid for optical photons, which for the most part propagate through (clear) glass unimpeded, without undergoing any collisions. However, in industrial problems, glass temperatures are much higher than room temperature, and at such temperatures, the mean free paths of photons at frequencies that carry most of the radiative energy are indeed short. Thus, despite physical intuition concerning optical photons, a typical value of ε in practical glass-annealing problems is indeed sufficiently small that asymptotic expansions of the type discussed in this paper are relevant.

Finally, we comment on the quality of the SP_N solutions that we have obtained numerically. Generally, the SP_N solutions are in very good agreement with the solution of the original radiative heat transfer equations. In particular, the SP_3 solution coincides remarkably well with the radiative transfer solution, even in the presence of a discontinuity in the opacities. Also, the SP_N models significantly outperform the standard Rosseland approximation, which has been used for a long time as an approximation for optically thick,

diffusive problems. We also note that, in contrast to the Rosseland equation, the SP_N equations give good results even when the regime is not so diffusive. The numerical SP_N solution is somewhat more costly than the solution of the Rosseland approximation, but *much* less costly than the full radiative heat transfer problem. Finally, the SP_N systems of diffusion equations can be solved by widely used, conventional software packages.

REFERENCES

1. P. S. Brantley and E. Larsen. The simplified P_3 approximation, *Nucl. Sci. Eng.* **134**, 1 (2000).
2. C. Cercignani. *The Boltzmann Equation and Its Applications* (Springer, 1988).
3. B. Dubroca. *Thèse d'Etat*, Dept. of Mathematics, University of Bordeaux, 2000.
4. E. M. Gelbard. Simplified spherical harmonics equations and their use in shielding problems, *WAPD-T-1182* (*Bettis Atomic Power Laboratory*, 1961).
5. R. Howell and J. R. Siegel. *Thermal Radiation Heat Transfer*, 3rd ed. (Taylor & Francis, 1992).
6. A. Klar and C. Schmeiser. Numerical passage from radiative heat transfer to nonlinear diffusion models, *MMMAS* **11**, 749–767 (2001).
7. A. Klar and N. Siedow. Boundary layers and domain decomposition for radiative heat transfer and diffusion equations: Applications to glass manufacturing processes, *Eur. J. Appl. Math.* **9–4**, 351–372 (1998).
8. E. Larsen, J. E. Morel, and J. M. McGhee. Asymptotic derivation of the multigroup P_1 and simplified P_N equations with anisotropic scattering, *Nucl. Sci. Eng.* **123**, 328 (1996).
9. E. Larsen, G. Pomraning, and V. C. Badham. Asymptotic analysis of radiative transfer problems, *J. Quant. Spectr. Radiative Transfer* **29**, 285–310 (1983).
10. C. L. Leakeas and E. W. Larsen. Generalized Fokker-Planck approximations of particle transport with highly forward-peaked scattering, *Nucl. Sci. Eng.* **137**, 236 (2001).
11. F. T. Lentes and N. Siedow. Three-dimensional radiative heat transfer in glass cooling processes, *Glastech. Ber. Glass Sci. Technol.* **72**, 188–196 (1999).
12. M. F. Modest. *Radiative Heat Transfer* (McGraw-Hill, 1993).
13. G. Pomraning. Initial and boundary conditions for equilibrium diffusion theory, *J. Quant. Spectr. Radiative Transfer* **36**, 69 (1986).
14. G. C. Pomraning. Asymptotic and variational derivations of the simplified P_N equations, *Ann. Nuclear Energy* **20**, 623 (1993).
15. D. I. Tomašević and E. W. Larsen. The simplified P_2 approximation, *Nucl. Sci. Eng.* **122**, 309–325 (1996).
16. R. Viskanta and E. E. Anderson. Heat transfer in semitransparent solids, *Adv. Heat Transfer* **11**, 318 (1975).